Hindawi
Journal of Advanced Transportation
Volume 2020, Article ID 6520861, 16 pages
https://doi.org/10.1155/2020/6520861

Research Article

A Car-Following Driver Model Capable of Retaining Naturalistic Driving Styles

Jie Hu and Sheng Luo

College of Computer Science and Artificial Intelligence, Wenzhou University, Wenzhou, Zhejiang 325000, China

Correspondence should be addressed to Sheng Luo; ls2008@wzu.edu.cn

Received 18 June 2019; Revised 2 December 2019; Accepted 11 December 2019; Published 21 January 2020

Academic Editor: Shamsunnahar Yasmin

The modeling of car-following behavior is an attractive research topic in traffic simulation and intelligent transportation. The driver plays an important role in car following but is ignored by most car-following models. This paper presents a novel car-following driver model, which can retain aspects of human driving styles. First, simulated car-following data are generated by using the speed control driver model and the real-world driving behavior data if the real-world car-following data are not available. Then, the car-following driver model is established by imitating human driving maneuver during real-world car following. This is accomplished by using a neural network-based learning control paradigm and car-following data. Finally, the FTP-72 driving cycle is borrowed as the speed profile of the leading vehicle for the model test. The driving style is quantitatively analyzed by A_{ESD}. The results show that the proposed car-following driver model is capable of retaining the naturalistic driving styles while well accomplishing the car-following task with the error of relative distance mostly less than 5 meters for every driving styles.

1. Introduction

Car-following behavior is common in real-world driving, and its modeling has been an important research topic in traffic simulation and vehicle technology. In the car-following task, the following vehicle is required to minimize the tracking errors in relative speed and distance with a leading vehicle. The strategies employed may vary from person to person. The car-following model (CFM) has been studied for decades. It mainly relies on mathematical formulas and is derived from traffic flow theory. The General Motors (GM) model is a good example, dating from the 1950s [1], and the Gipps model is probably the most widely adopted in microsimulation [2]. Unfortunately, the role of the driver is neglected or ignored in almost all CFMs, and consequently, no driving style is exhibited.

Car-following modeling has been an attractive research topic for decades. The Gazis–Herman–Rothery (GHR) model was proposed in 1958 at the General Motors research laboratory [3] and was hereafter named as the GM model. This model considers acceleration as a function of the leading vehicle's speed, relative speed, relative distance, and driver reaction time. The collision avoidance (CA) model [4] describes the safe following distance as a function of the speeds of the leading and the follower vehicles and the driver's reaction time. The Gipps model [2] is based on the CA model and is widely used for microscopic traffic simulation. Many control approaches are also applied to develop car-following models. An application of fuzzy logic to the GHR model was reported in [4]. A back-propagation neural network was applied to develop a car-following model by Jia et al. [5]. A comprehensive review of car-following modeling was presented by Brackstone and McDonald [6].

In recent years, some works focused on the driver's behavior in the car-following process [7–12]. In 1998, Boer and Hoedemaeker [13] proposed a hierarchical driver modeling framework, which took task scheduling, attention management, and performance into consideration. They pointed out that a neural net with proper measurable input variables may be an alternative solution to characterizing

human driver behavior and modeling in traffic simulation [14]. Zhong et al. [15] modeled the intelligent car-following model using Gaussian random variables as the parameters to perform a probabilistic sensitivity analysis based on the Kullback–Liebler dissimilarity measure in order to limit the number of parameters requiring value estimation to those yielding the greatest performance improvement relative to default parameter values. In [16], human-like car-following controllers without considering vehicle dynamics are developed using deterministic policy gradient by learning from naturalistic human driving data. Khodayari et al. [17] proposed a modified car-following model, which included human driver effects, such as driver's reaction time. These and other unmentioned works have made significant contributions to the advancement to the understanding and modeling of driver's behavior during car-following. One issue that is rarely addressed is the retaining of human's naturalistic driving styles, which is however important for car-following models.

The objective of this work is to develop a car-following driver modeling scheme that is capable of retaining the original human driving styles. We propose to establish the style-retaining Car-Following Driver Model (CFDM) by imitating human driving behaviors. The CFDM is designed to track the relative speed and distance with a personal sustainable level. Although ignored by most car-following models, the driver plays an important role in car following and should be taken into account in the modeling.

The CFDM to be developed in this work is different from the CFM in two aspects: (1) CFDM models the relationship between the follower driver's operations on the gas/brake pedal and the relative speed/distance, while the CFM replicates the relationship between the follower vehicle's speed or acceleration and the relative speed or distance; therefore, CFDM is a driver model while the role of the driver is neglected in CFM. Hence, CFM is not directly applicable in unmanned vehicles. (2) More importantly, CFDM can retain a particular driving style, while the CFM cannot.

We propose to employ the neural network-based learning control paradigm and the real-world car-following data (CFD) to make the style-retained driver modeling possible. Because of the personality of driving behaviors, the car-following process is individual and complex. Hence, the modeling of car following is analytically difficult. It is noticed that a driver improves his or her driving maneuver through repeated practices. It is thus possible to establish the style-retained CFDM by gradually imitating human driving behaviors during real-world driving. More specifically, the direct inverse modeling approach [18] is employed, and the imitation of driving behavior is modeled using locally designed neural networks.

To the best knowledge of the authors, there are three main contributions in this paper: (1) This paper proposes a novel method for modeling CFDM capable of retaining naturalistic driving styles. (2) The proposed CFDM can well accomplish the car-following task. (3) Minor diversities exist among CFDMs of the same driving style. Each CFDM displays the unique behavior of the driver.

The remainder of this paper is organized as follows. Section 2 gives a brief review of the speed-tracking driver model. Driving behavior data and energy spectrum density are used in establishing and evaluating this model. Section 3 introduces the process for generating simulated car-following data. In Section 4, a novel car-following model is developed. The simulated car-following test procedure and results are represented in Section 5. In Section 6, the results of the tests are analyzed. Conclusions and future work are given in Section 7.

2. Review on STDM, DBD, and ESD

The speed-tracking driver model (STDM) is established based on the DBD and is applied to generate the simulated car-following data. In addition, the energy spectrum density (ESD) is used to evaluate the aggressiveness of driving behavior. These issues are reviewed as follows.

2.1. STDM. In our previous work [19], a STDM was established by using a neural network, as shown in Figure 1. A learning-based control approach is used to learn the human operations on the block diagram of the driver modeling process. Adapting to become an inverse model of the vehicle, the driver modeling is accomplished by the distal guidance learning.

2.2. Driving Behavior Data (DBD). Collected from an instrumented vehicle by a motor company, DBD take account into various combinations of road situations (highway and city), driving styles (mild, moderate, and aggressive), and vehicle types (Fiesta or Escort). Many quantities are recorded in DBD, including vehicle speed (VS), throttle position (TP), brake pressure (BP), and engine speed. 36 classified DBD samples are used in this work for driver modeling. Examples of the DBD samples are shown in Figure 2.

In the longitudinal driving situation, the driving behavior is mainly represented by throttle position (TP) [20]. Figure 3 gives a summary view of TP time series of 18 DBD samples on city roads, where each column represents the time series of a certain driver. As shown on the x-axis, No. 1 to No. 6 was originally classified as the mild, while No. 7 to No. 12 was classified as the moderate and No. 13 to No. 18 was classified as the aggressive. It is obvious that TP varies widely among different driving styles.

2.3. Energy Spectral Density (ESD). The ESD is applied to quantitatively evaluate the aggressiveness of driving behavior [20]. ESD describes the energy distribution of a time series with the frequency. The spectral density $\phi(w)$ of a time series with finite energy $f(t)$ is the square of the amplitude of its continuous Fourier transform $F(w)$ [21]:

$$\phi(w) = \left| \frac{1}{\sqrt{2\pi}} \int_{-\infty}^{\infty} f(t) e^{-iwt} \mathrm{d}t \right|^2 = \frac{F(w) F^*(w)}{2\pi}, \quad (1)$$

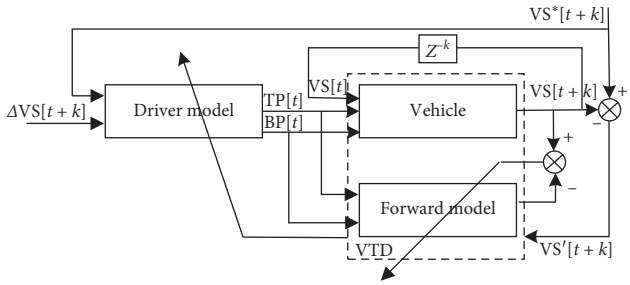

Figure 1: Speed-tracking driver modeling based on learning control.

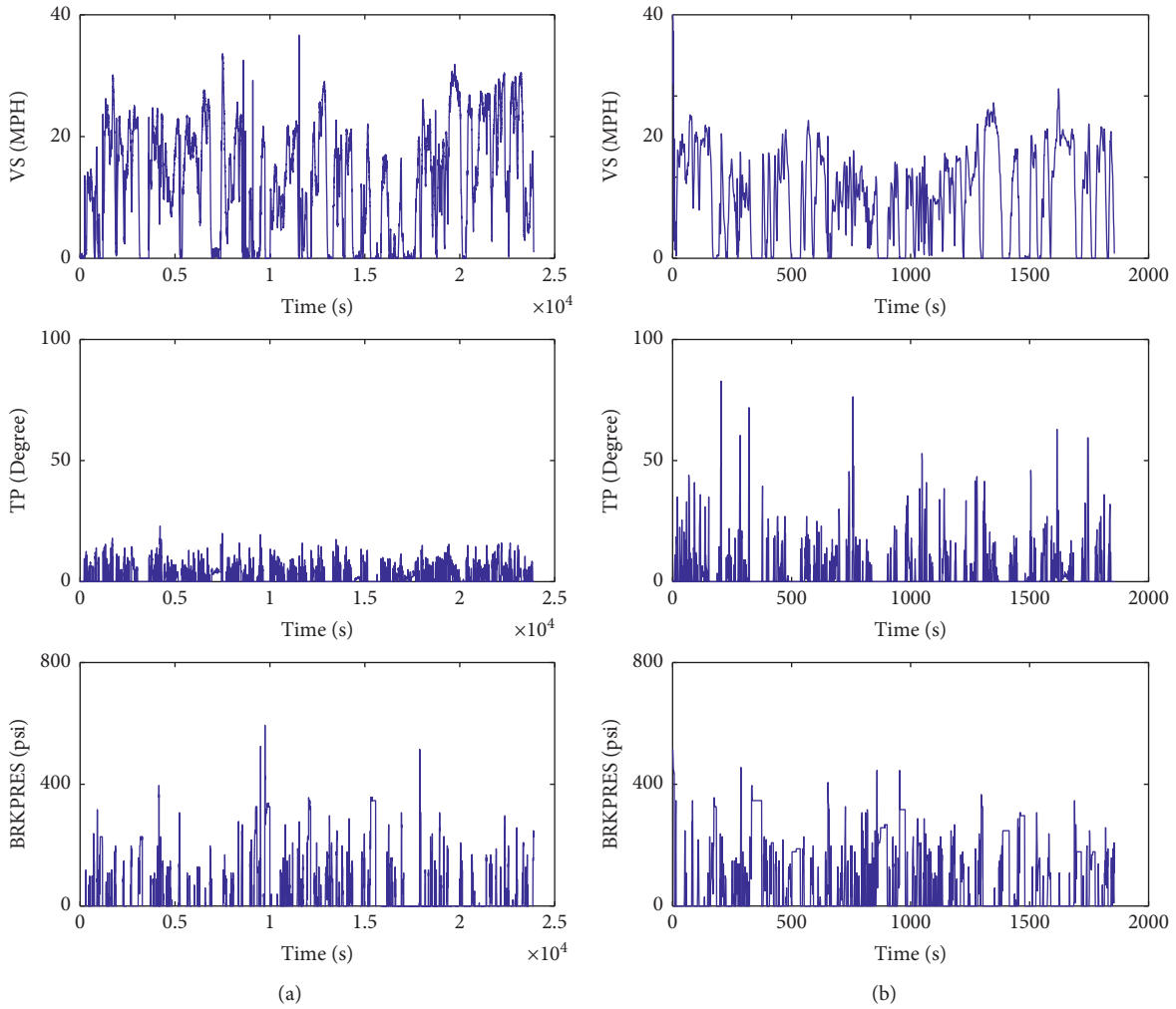

Figure 2: Driving behavior data examples. (a) Mild-city. (b) Aggressive-highway.

where $F(w)$ is the continuous Fourier transform of $f(t)$ and w is the angular frequency. $F^*(w)$ is a conjugate function of $F(w)$. Thus, the ESD of the discrete time series of TP in this research is

$$D(w) = \left| \frac{1}{\sqrt{2\pi}} \sum_{n=-\infty}^{\infty} f_n e^{-iwn} \right|^2. \quad (2)$$

After converting to the frequency domain, $D(w)$ is used to characterize the variance of car-following behavior.

3. Simulated Car-Following Data (SCD)

SCD are generated in case real-world car-following data (RCD) are not available. Car-following data are essential for

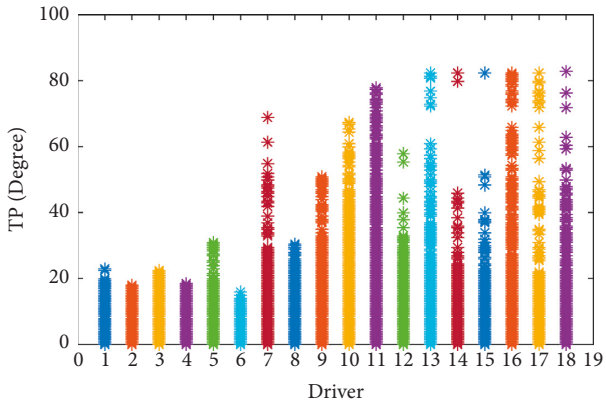

Figure 3: TP distribution of 18 DBD on city roads.

car-following modeling. However, it may not be available due to the fact that data collecting may consume extra manpower and material resources unless originally arranged. On the other hand, real-world speed-tracking DBD are routinely collected by automobile companies and is thus available. We propose to generate simulated car-following data by using the real-world DBD.

SCD generation is implemented by emulating a real-world car-following scene. The car-following behavior can be described as the longitudinal action of a driver when following another car. The relative distance is determined by the follower's speed with respect to his/her aggressiveness and the leading vehicle's behavior. Figure 4 shows the car-following scene with necessary variables for SCD generation, where V_F (in mile/h) denotes the speed of the follower, V_L (in mile/h) denotes the speed of the leading vehicle, and V_R (in m) denotes the relative distance between these two vehicles.

Two sets of SCD are generated by using the same process for driver modeling and model testing, namely, the training SCD and the testing SCD. The only difference lies in the speed profile of the leading vehicle. In generating the training SCD, the actual speed in each DBD sample is used as the speed profile of the leading vehicle, whereas the speed profile of the FTP-72 is used for generating the test SCD.

3.1. Generation of SCD. As reviewed in the Section 2, the STDM is capable of imitating and reproducing the driving behavior of the original human driver in the longitudinal driving situation; for this reason, we propose to employ the STDM as a virtual driver to generate SCD.

The follower vehicle is assumed to be operated by a virtual driver (*Vir*Driver), or a STDM, to follow a leading vehicle when it is driven with a certain speed profile, i.e., the profile used for real-world vehicle testing or the standard driving cycle test.

The SCD generation proceeds as shown in Figure 5 and is conducted recursively. The *Vir*Driver issues appropriate TP or BP operations according to the desired vehicle speed $V_{FD}[t]$ and current vehicle speed $V_F[t]$, which results in the actual vehicle speed at next moment $V_F[t+1]$. Then, the relative distance D_R is obtained by the integral of the

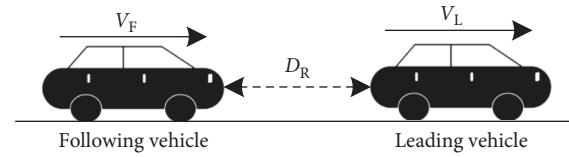

Figure 4: Car-following scene.

difference between the speed of the leading vehicle V_L and the follower V_F. A distance-to-speed conversion (DSC) module is designed to transform the relative distance D_R to the desired follower speed at the next moment, $V_{Fd}[t+1]$. The actual speed of the real-world DBD is adopted as the speed profile of the leading vehicle, and the resulted follower's TP/BP operations, vehicle speed, and the relative distance constitute the simulated car-following data.

3.2. DSC. A DSC mechanism is proposed to convert the relative distance to the desired speed V_{Fd} (in mile/h) for the follower vehicle. It is found that the time-headway (THW) is consistent with drivers and is constant over a range of speeds [22]. THW represents the time available for the driver to reach the same level of deceleration as the leading vehicle in case it brakes [23] and is widely used in risk measurement and driving-assisting system design [24]. Based on the assumption that THW tends to be constant and is subject to Gaussian distribution for each driver, V_{Fd} is defined by (3), where THW and σ vary from driver to driver, depending on their driving styles:

$$VF_{Fd} \sim N\left(\frac{D_r}{\text{THW}}, \sigma^2\right). \quad (3)$$

4. Car-Following Driver Modeling

The CFDM is established by imitating human driver behavior. This is accomplished by using the learning control paradigm. By adapting to become an inverse model of the vehicle behavior, the follower driver (model) and the vehicle (model) work together to form a closed-loop control system.

The modeling of CFDM is illustrated in Figure 6, where the CFDM is learnt and modified by using the direct inverse modeling approach [18]. Because of the causes of speed changes, the actually applied TP or BP forms the desired output for the CFDM. The integral of the difference between the vehicle speed of follower V_F and the leader V_L forms the relative distance and serves as the input to CFDM. To some extent, this is similar to inversing the roles of the input and the output of the follower vehicle. A neural network is utilized to mimic human car-following behaviors, i.e., TP/BP operation during real-world driving, by learning this inverse relationship. To deal with the possible drastic variations on a local or intermediate scale within the driving behavior data, the B-spline neural network (BSNN) is employed to implement the car-following driver model.

As shown in Figure 7, BSNN is a locally designed feed-forward neural network composed of B-spline basis functions [25, 26]. The output of a BSNN is represented as

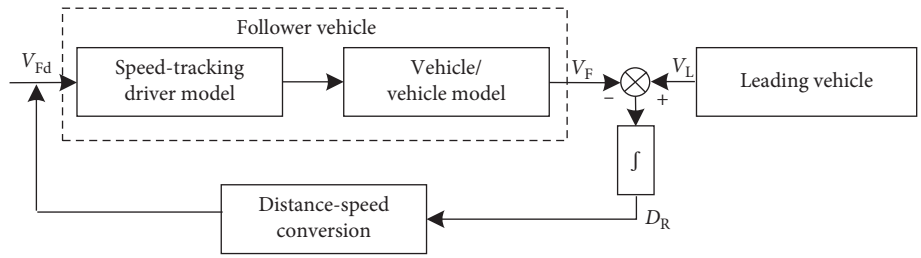

Figure 5: Simulated car-following data (SCD) generation.

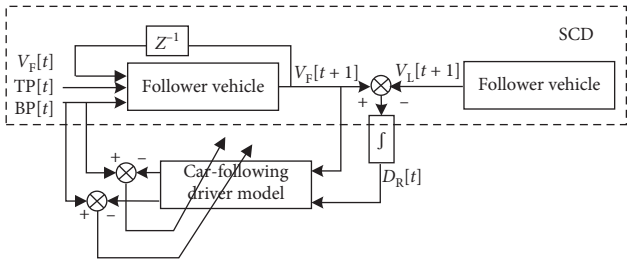

Figure 6: Car-following driver modeling based on direct inverse modeling approach.

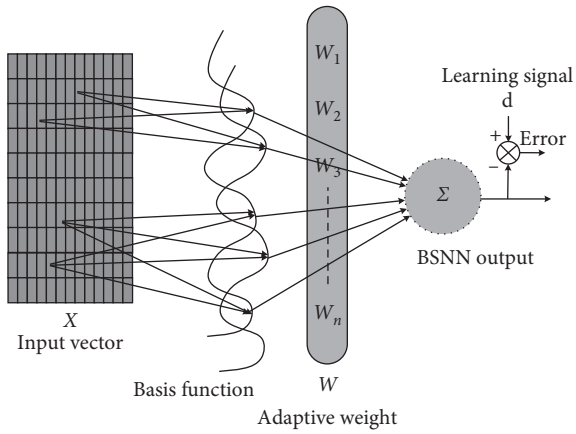

Figure 7: B-spline neural network.

$$y_k = f(x_k) = \sum_{i=1}^{N} w_i b_q^i(x), \tag{4}$$

where x_k and y_k are the input and output of the network, respectively, w_i is the weight attached to the ith basis function, and $b_q^i(x)$ is defined as the ith basis function of order q.

Each B-spline basis function is composed of q polynomial segments. A simple and stable recursive relationship exists to evaluate the membership of a B-spline basis function of order q, shown as (5) and (6):

$$b_q^i(x) = \left(\frac{x-\lambda_i}{\lambda_{i+q}-\lambda_i}\right) b_{q-1}^i(x) + \left(\frac{\lambda_{i+q+1}-x}{\lambda_{i+q+1}-\lambda_{i+1}}\right) b_{q-1}^{i+1}(x), \tag{5}$$

$$b_0^i(x) = \begin{cases} 1, & x \in I_i, \\ 0, & \text{otherwise}, \end{cases} \tag{6}$$

where $b_q^i(x)$ is the ith basis function of order q, λ_i is the ith knot, and I_i is the ith interval.

5. Car-Following Test Simulation

To verify the effectiveness of the proposed scheme, the established CFDM is applied to the car-following test simulation as shown in Figure 8. In order to improve the transient response, a regular proportion and derivative (PD) controller is usually employed as an auxiliary controller [27] in learning control. It also helps in handling hazardous situations such as avoiding crashes when two vehicles are too close.

The leading vehicle and the traffic conditions are important factors affecting the follower driver's behavior [1, 27, 28]. In order to evaluate the car-following performance on an equal base, these two factors should be kept unchanged as much as possible. As a well-known driving cycle test, the FTP-72 is used here as the speed profile of the leading vehicle.

The car-following test proceeds as follows:

(1) The leading vehicle adopts the FTP-72 speed profile as its current vehicle speed V_L and then calculates the relative distance D_R by the integral of the difference between the vehicle of the follower and the leading vehicle, as defined by (7).

(2) Determine the output of the car-following driver model, $TP_m[t]$ or $BP_m[t]$, according to the current leading speed $V_L[t]$ and relative distance $D_R[t]$; meanwhile, obtain the output of the PD controller, $TP_a[t]$ or $BP_a[t]$, according to current relative distance $D_R[t]$. The actual applied TP[t] or BP[t] is their summation as defined by (8) to (11):

$$D_R[t] = \int_0^{t-1} (V_L[t] - V_F[t])\mathrm{d}T, \tag{7}$$

$$\{TP_m[t+1], BP_m[t+1]\} = \mathrm{BSNN}(V_L[t], D_R[t]), \tag{8}$$

$$\{TP_a[t+1], BP_a[t+1]\} = \mathrm{PD}(D_R[t], \Delta D_R[t]), \tag{9}$$

$$TP[t+1] = TP_m[t+1] + TP_a[t+1], \tag{10}$$

$$BP[t+1] = BP_m[t+1] + BP_a[t+1]. \tag{11}$$

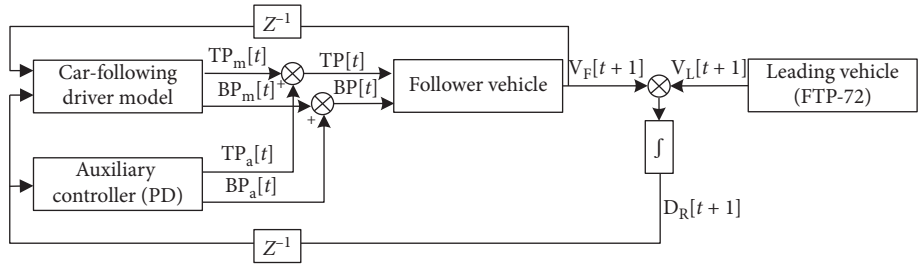

Figure 8: Car-following test simulation.

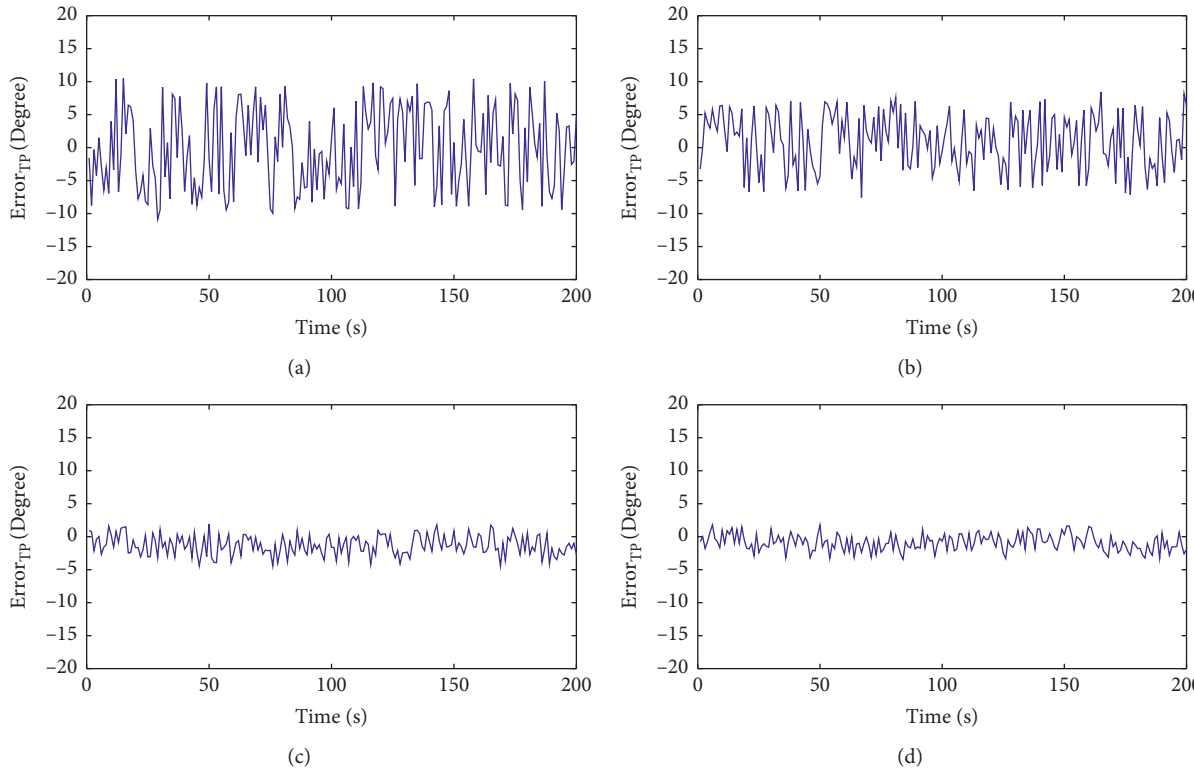

Figure 9: Error of TP during training CFDM after 5 (a), 10 (b), 40 (c), and 80 (d) epochs.

(3) The vehicle model outputs follower's speed $V_F[t+1]$, accordingly.

(4) Repeat steps 1 to 3 recursively until the entire driving cycle speed profile is accomplished.

Since a *Vir*Driver can be implemented by using the proposed car-following driver model under various vehicle test conditions, the car-following performance can be demonstrated for various driving styles and road situations.

6. Results

To verify the proposed scheme, simulations have been accomplished by using the 36 DBD samples as described in Section 2. Firstly, a car-following driver model is established for each DBD sample, which results in 36 CFDMs. Secondly, each established CFDM is applied to the car-following test simulation, where the leading vehicle speed profile is adopted from the FTP-72 with the same road type as that in DBD.

Several issues are considered in evaluating the car-following performance: (A) training error of CFDM; (B) the effect of the follower driving style; (C) sensitivity analysis for the order of B-spline function; (D) consistency with the original data, and (E) diversity and similarity within the same driving style.

6.1. Training Error of CFDM. The weights of CFDM is learnt and modified by using direct inverse modeling approach as shown in Figure 6. Figures 9 and 10 show the error of TP and BP after being tuned for 5, 10, 40, and 80 epochs.

As shown in Figure 9, the error of TP lies in the range of [−10, +10] degrees after 5 epochs, then [−5, +10] degrees after 10 epochs, and finally decreases to [−2, +2] degrees. The performance of BP is the same as shown in Figure 10. The

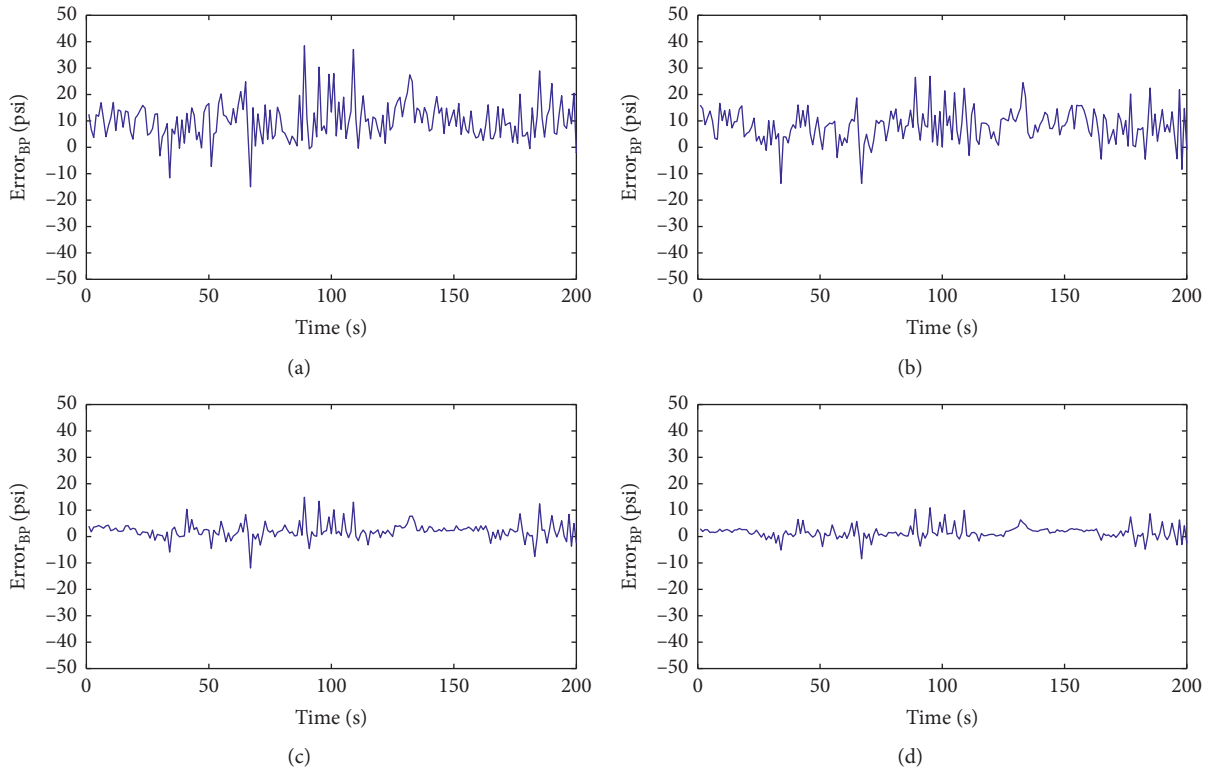

Figure 10: Error of BP during training CFDM after 5 (a), 10 (b), 40 (c), and 80 (d) epochs.

error of BP finally decreases to [−10, 10] psi after 80 epochs. Obviously, the error of TP and BP is continuously becoming smaller as far as the tuning of CFDM is being conducted and eventually converges.

6.2. Effect of the Follower Driving Style. We consider 3 driving styles and 2 road conditions, which forms 6 combinations, namely, Aggressive-City, Moderate-City, Mild-City, Aggressive-Highway, Moderate-Highway, and Mild-Highway. Figures 11–16 show the car-following performance of one CFDM for each combination, where subplots (a's) show the vehicle speed of the leading and the follower, subplots (b's) show the TP time series of the follower, and subplots (c's) show the error of the relative distance between the car-following test result and the test SCD, i.e., Dis_Error.

As can be seen in subplots (a's) and (c's), all follower vehicles track the leading vehicle's speed quite well, except for a slight lag. The resulted error in relative distance is acceptable compared with the original SCD. It is for the most part less than 5 meters. Subplots (b's) show that distinguished diversity exists in the TP operations among drivers of different driving styles when following the same leading vehicle, either on the city road or highway.

Figure 17 demonstrates the car-following performance during the acceleration and deceleration process on city roads, which are parts of the FTP-72 driving cycle. As shown in Figure 17(a), the aggressive driver accelerates more rapidly and follows the leading vehicle better than the other due to his/her aggressive personality. In Figure 17(b) , the leading vehicle brakes to stop. The mild driver tends to decelerate smoothly while the aggressive driver is more likely to brake sharply.

Each driver has a unique TP time series even when drivers follow the same leading vehicle. The ESD and the variance of TP are thus calculated for evaluating the car-following driving behaviors. Table 1 shows these two indices applied to the TP series of following cases: (1) σ_{TP}, variance of TP; (2) A_{ESD}, average of ESD of TP. Obviously, σ_{TP} and A_{ESD} can both roughly distinguish the three styles, where A_{ESD} is better for characterizing the TP distribution among the styles. A_{ESD} is thus selected as the feature of car-following driving style clustering.

In order to visually demonstrate the car-following driving style reproduction of the CFDM, a K-means algorithm is applied to cluster these two groups of 36 results. The clustering results are shown in Figure 18, where dotted horizontal lines from the top to bottom represent clustering centres of the aggressive, moderate, and mild drivers, respectively.

These centres are 359.75, 307.05, and 244.15 for city and 1118.2, 945.7, and 815.5 for highway. Every sample is fitted to its original experiential classification, which means the driving style is retained and the distinction between different styles are kept.

6.3. Sensitivity Analysis of the Order of B-Spline Function. To deal with the possible drastic variations on a local or intermediate scale within the driving behavior data, the BSNN is employed to implement the car-following driver model. It is then verified by the car-following test simulation

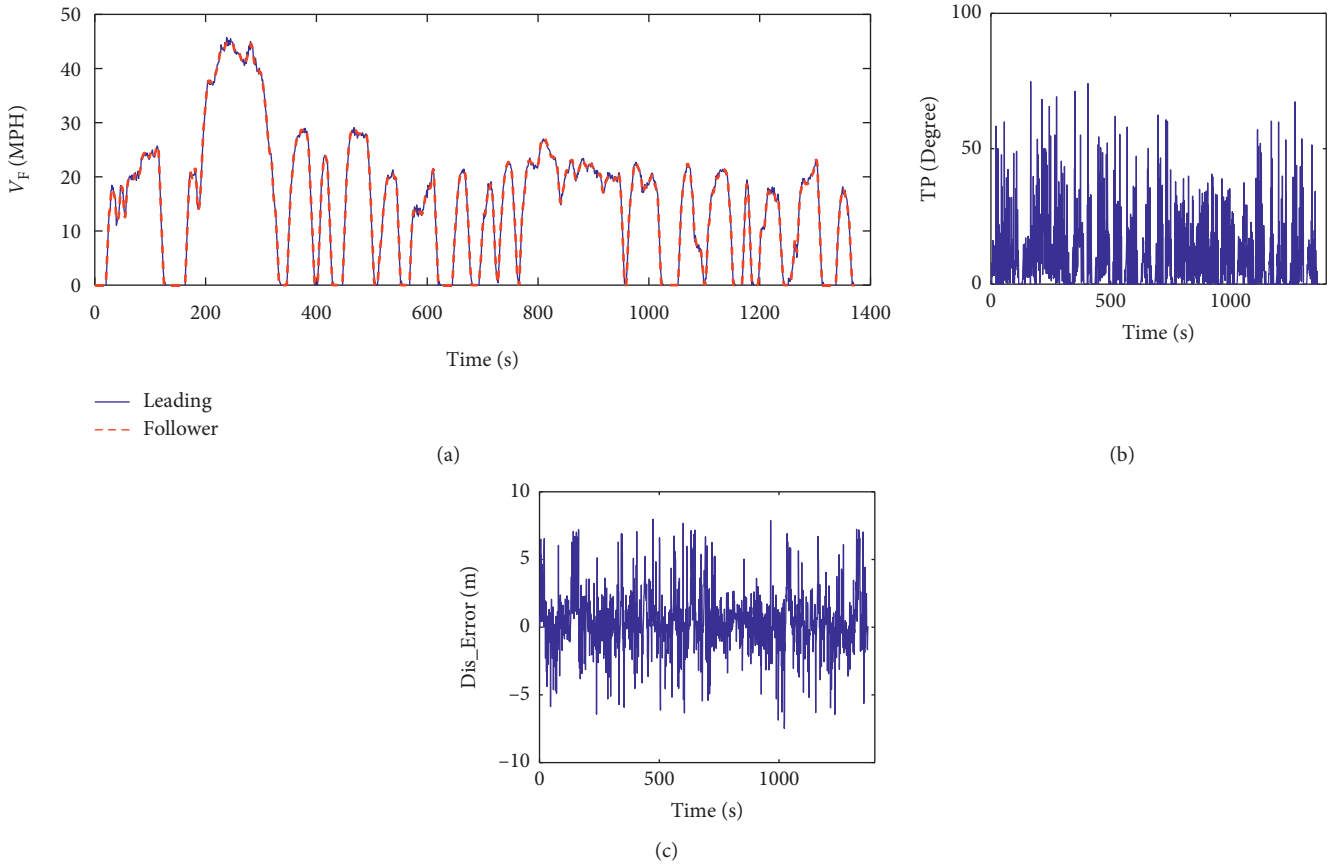

Figure 11: Car-following test: aggressive-city.

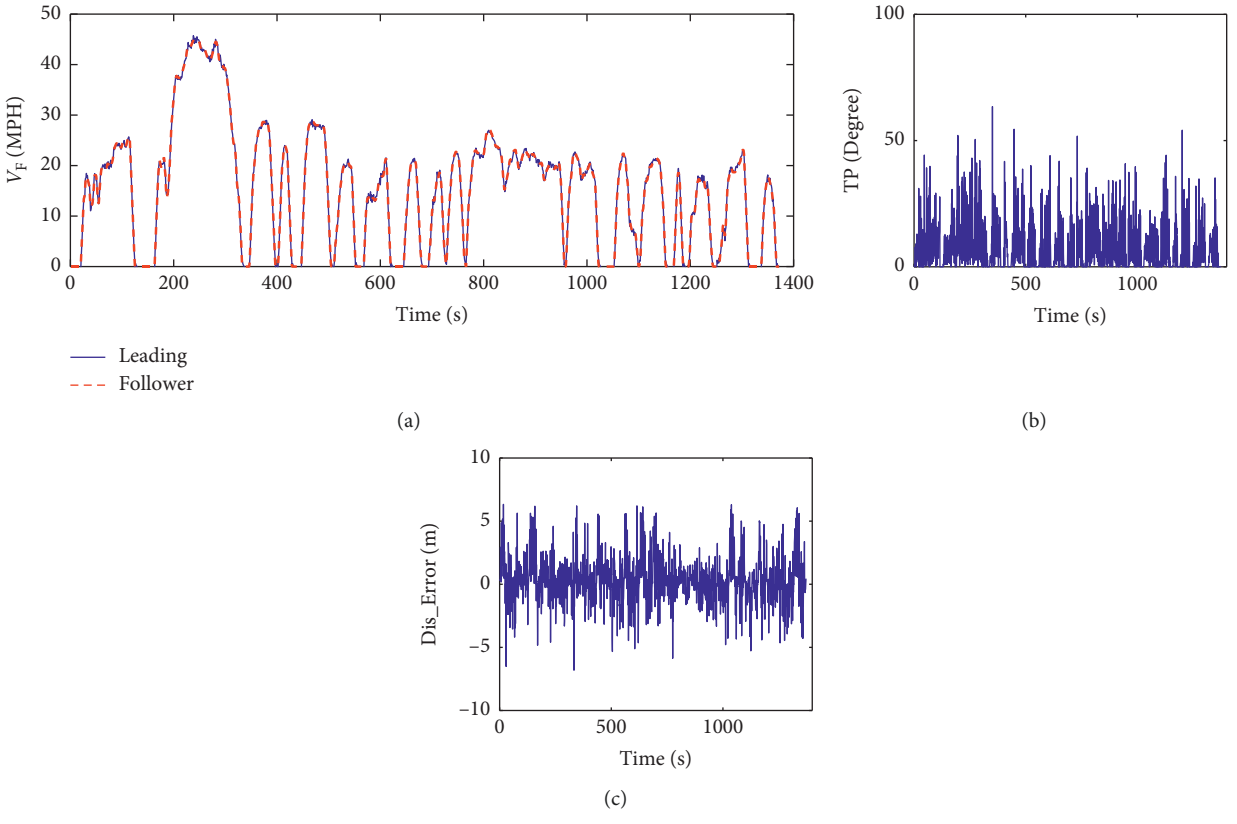

Figure 12: Car-following test: moderate-city.

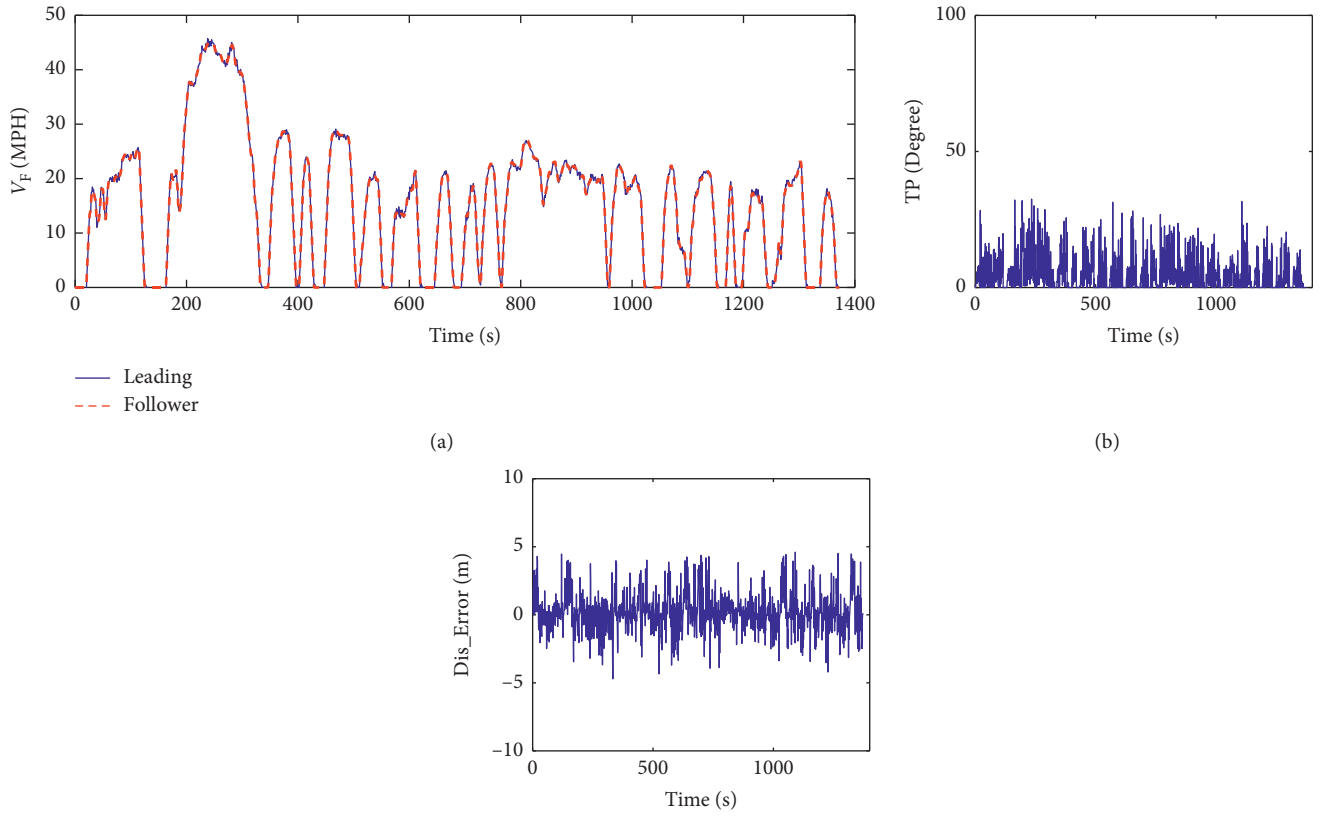

Figure 13: Car-following test: mild-city.

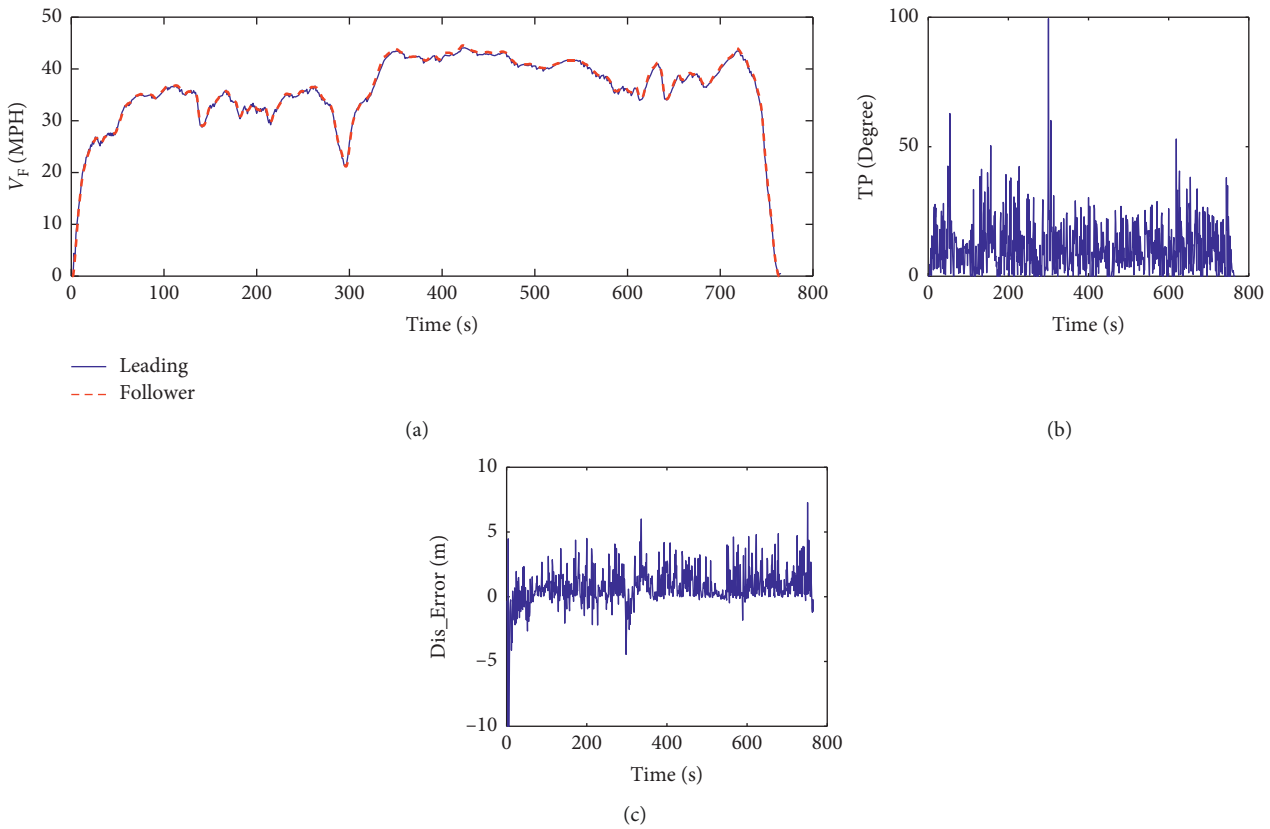

Figure 14: Car-following test: aggressive-highway.

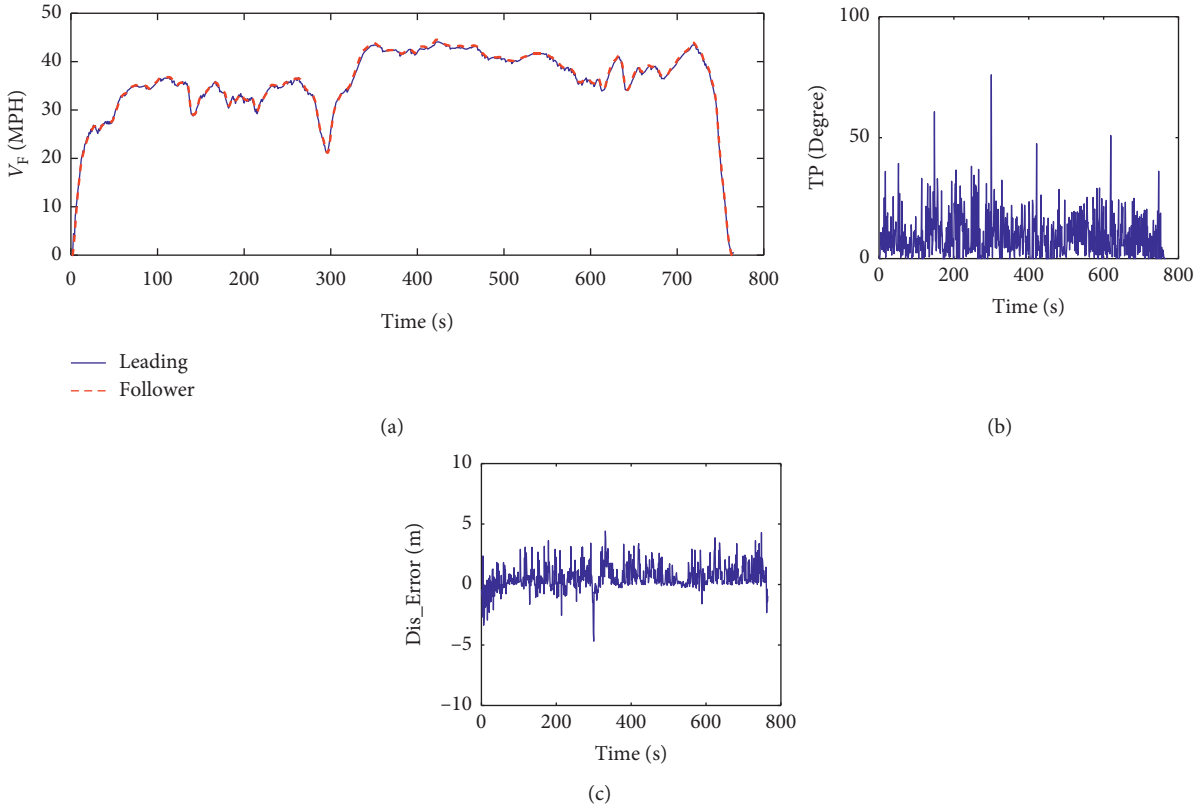

Figure 15: Car-following test: moderate-highway.

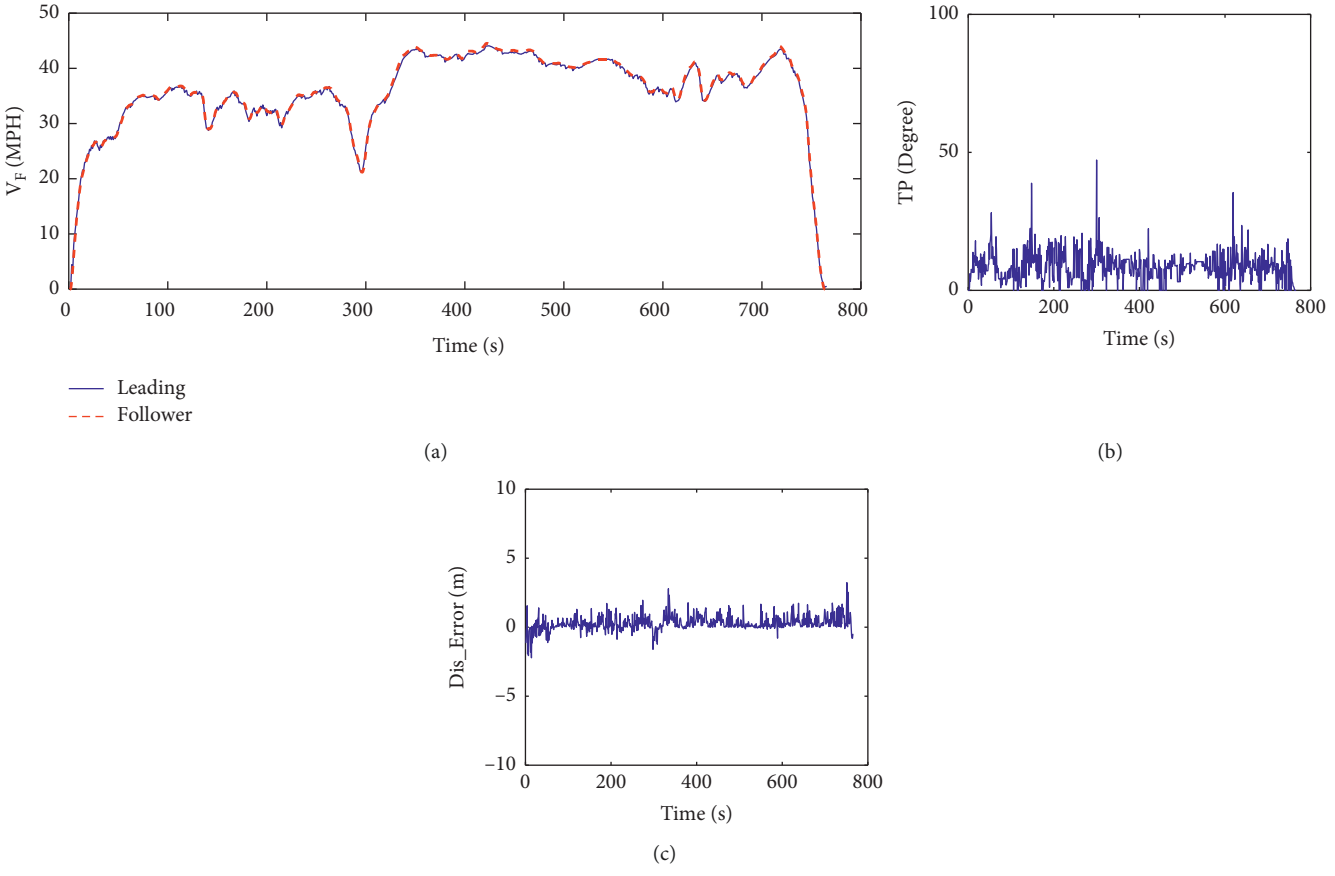

Figure 16: Car-following test: mild-highway.

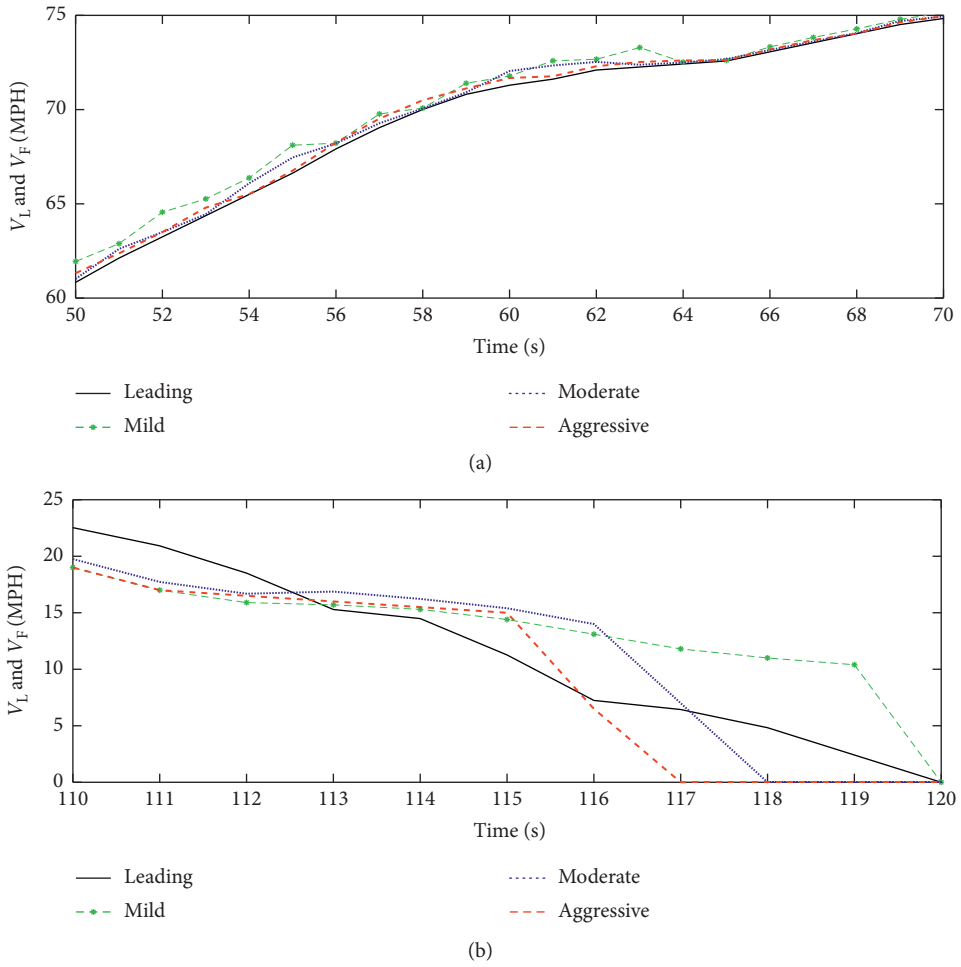

Figure 17: Two typical short time car-following behaviors in city roads.

Table 1: Indices of TP for city road and highway.

Driver	σ_{TP} (city)	A_{ESD} (city)	σ_{TP} (highway)	A_{ESD} (highway)
Mild #1	11.774	240.252	11.278	828.886
Mild #2	12.301	260.193	11.041	820.992
Mild #3	11.837	243.052	11.120	861.584
Mild #4	11.254	223.581	10.387	790.462
Mild #5	11.813	245.912	10.432	749.293
Mild #6	11.956	251.960	10.497	841.852
Mode #1	13.915	308.496	10.317	910.879
Mode #2	13.264	301.337	11.554	962.742
Mode #3	13.809	287.214	11.740	915.586
Mode #4	12.959	322.409	11.246	985.642
Mode #5	13.704	316.411	11.161	961.084
Mode #6	12.339	289.629	11.391	938.092
Agg #1	14.747	355.605	11.733	1144.425
Agg #2	14.905	361.851	12.782	1135.201
Agg #3	13.771	336.843	12.039	1058.622
Agg #4	15.064	391.851	13.173	1198.153
Agg #5	14.815	352.626	12.528	1090.364
Agg #6	14.128	323.874	12.803	1082.348

as shown in Figure 8. Sensitivity analysis should be conducted for the order of B-spline function and its impact on accuracy and instability.

Table 2 shows the car-following accuracy under different orders of B-spline function. The accuracy is indicated by

$$S_{err} = \frac{1}{m}\sum_{i=1}^{m} (\text{Dist\_Error})^2, \quad (12)$$

where m denotes the length of FTP-72. It is observed that the best performance of car following is obtained when the order of B-spline function is 3 both for the city road and highway. And the car-following accuracy deteriorates as the order increases beyond 3.

The stability of driving style under different orders of B-spline function is also studied. Figure 19 shows the resulted TP when the order q is 1, 3, and 6, respectively. It can be seen that the difference of driving style is not distinct among orders for the same style, while the driving styles are retained.

On the whole, the car-following accuracy is sensitive to the order of B-spline function and the driving style is not at all. This might be due to the fact that the car-following accuracy is highly relevant to the accuracy of the model itself, while the driving style is not.

6.4. Consistency with Original Car-Following Data. The consistency of the simulation results and original car-

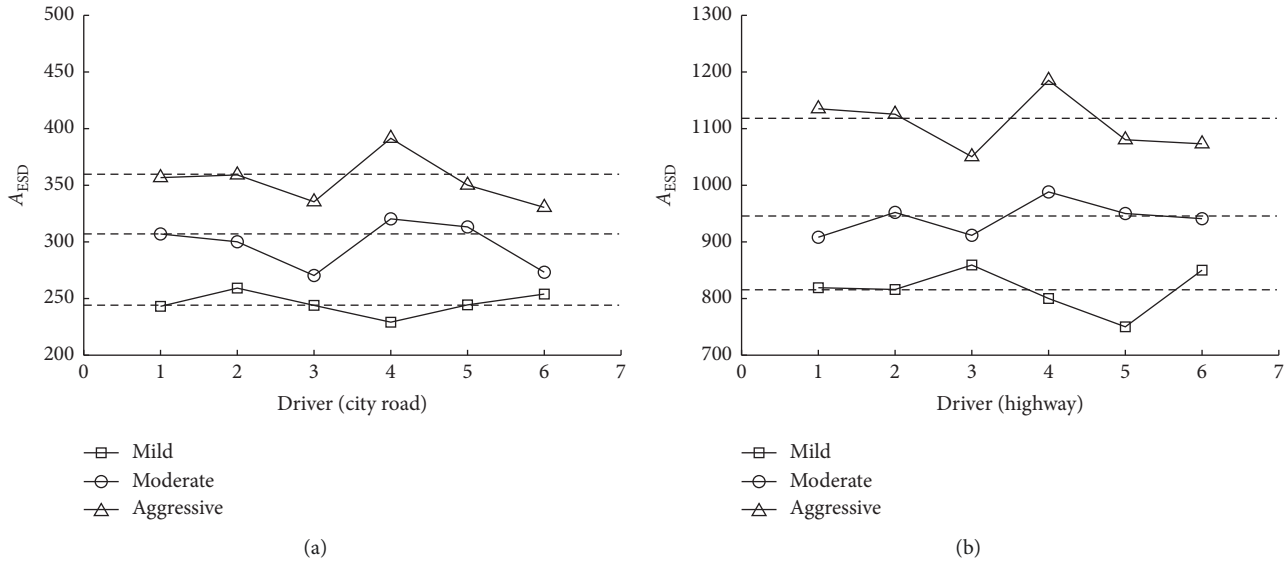

Figure 18: K-means clustering for A_{ESD} of TP in city road and highway (the dotted lines are the respective centres).

Table 2: Performance of car following under different q.

Order q	S_{err}	
	City road	Highway
1	25.28	19.71
2	15.21	10.34
3	9.32	3.20
4	12.41	4.32
5	13.90	5.03
6	13.86	4.59

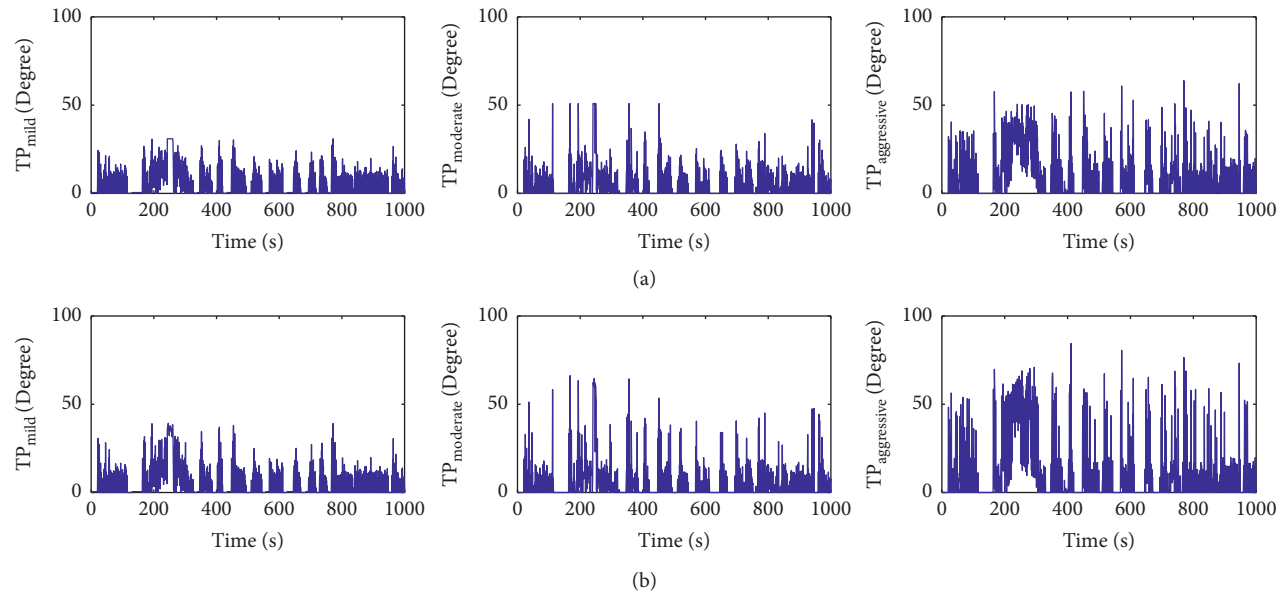

Figure 19: Continued.

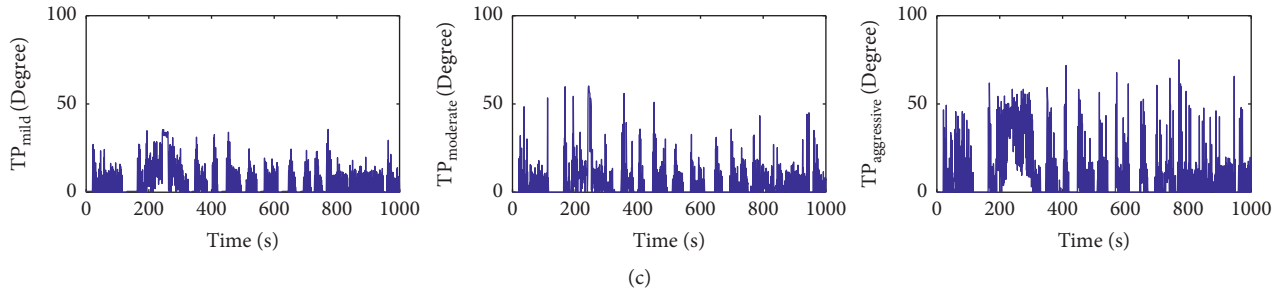

Figure 19: Resulted TP when the order of q is 1 (a), 3 (b), and 6 (c).

Table 3: Statistics on 36 car-following driver models on city road and highway.

	$\sigma_{err(VS)}$			$\sigma_{err(D_R)}$		
	min	max	mean	min	max	mean
Mild-city	2.421	3.107	2.793	4.337	7.796	5.581
Mode-city	2.864	5.587	4.172	5.053	7.295	6.499
Agg-city	2.357	4.276	3.342	4.148	7.84	5.663
Mild-highway	0.598	0.844	0.721	1.088	1.669	1.439
Mode-highway	0.950	1.637	1.496	1.517	3.316	2.542
Agg-highway	0.975	1.901	1.365	1.356	3.338	2.214

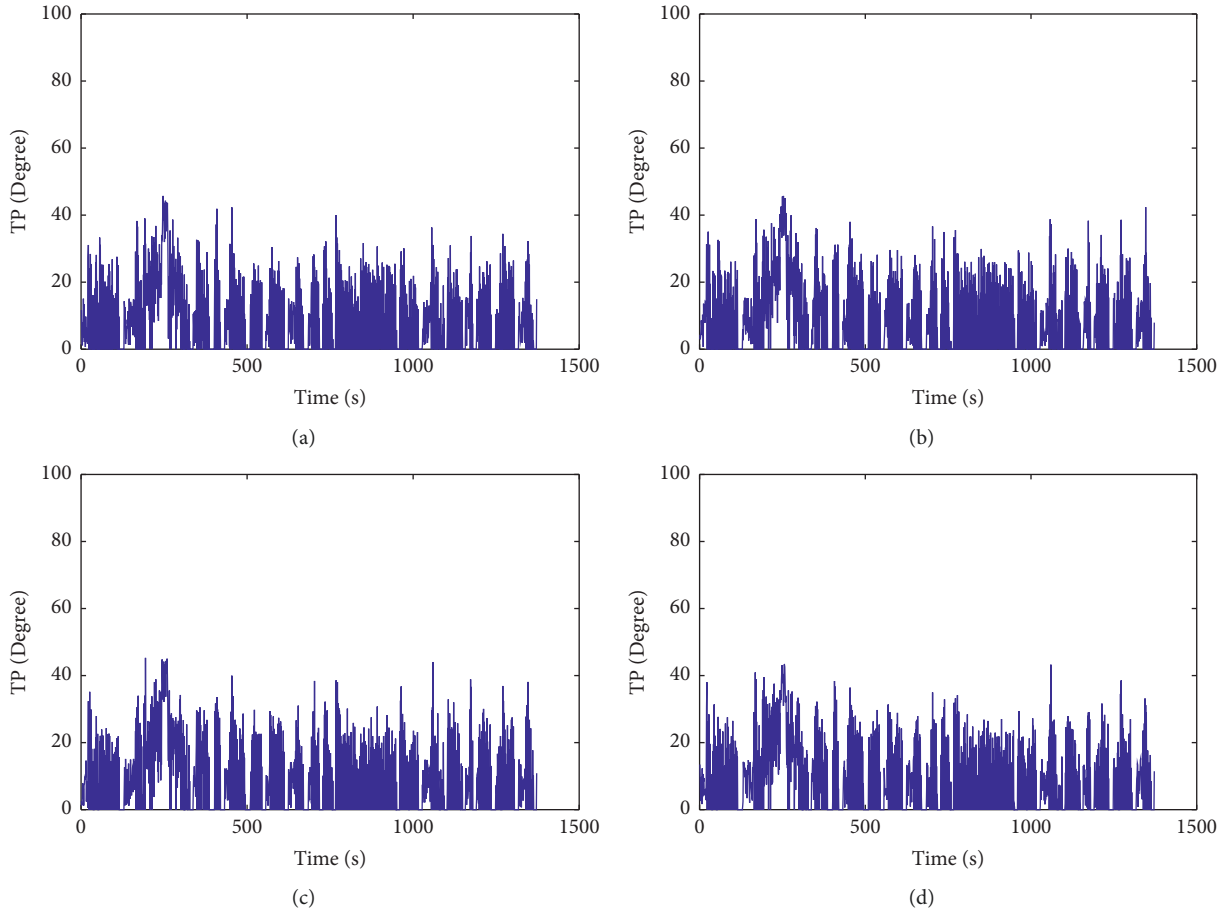

Figure 20: Car-following test on city roads: 4 mild CFDMs.

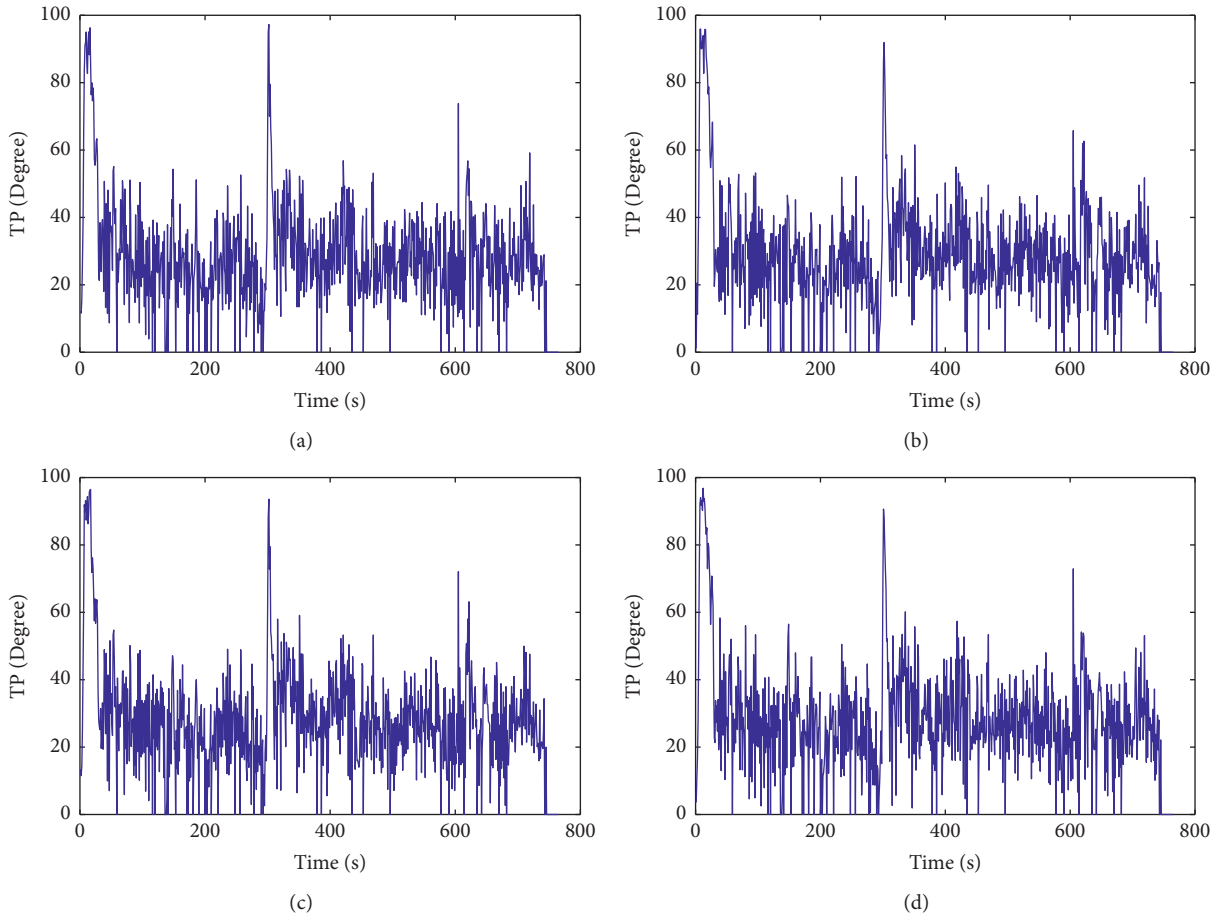

Figure 21: Car-following test on highway: 4 aggressive CFDMs.

following data is another important issue for evaluating the CFDM. Although the relative distance error is mostly less than 5 meters for every driving style, statistics on the variance of speed error and the variance of relative distance error are used to obtain a quantitative measure of this consistency. The variance of speed error shows the similarity between the CFDM and the original driver in operating the vehicle while the variance of relative distance error demonstrates the similarity in car-following performance.

Statistical of 36 results are shown in Table 3 with respect to the driving style and road condition. It can be seen from Table 2 that (1) The variance in all cases are small, which shows that every CFDM performs consistently with the original driver. (2) The variance is generally smaller on highways rather than on city roads. This is reasonable because city roads are usually more complicated than highways. (3) The $\sigma_{\mathrm{err}(\mathrm{VS})}$ and $\sigma_{\mathrm{err}(D_{\mathrm{R}})}$ are no much difference between different driving styles in each specific environment. Based on these three facts observed, a conclusion can be drawn that the CFDM performance is inconsistent with the original driving data.

6.5. Diversities of CFDMs of the Same Style. Figures 20 and 21 show the TP series of 4 CFDMs for mild drivers when conducting the car-following test on city roads and 4 CFDMs for aggressive drivers on highways. It can be seen that the CFDMs of the same driving style demonstrate similar driving behaviors, i.e., small magnitude in TPs with smooth changes for mild driver CFDMs and large magnitude TPs with sudden changes for CFDMs for aggressive drivers. However, minor diversities exist even though of the same driving style. Each CFDM displays the unique behavior of the driver.

7. Conclusions

Style-retained car-following driver modeling is studied in this paper. We establish a car-following driver model by imitating human driving behaviors. This is accomplished by using a neural network-based learning control paradigm and the car-following data. We also generate simulated car-following driving data by employing the speed-tracking driver in case that the real-world car-following driving data are not available. Finally, FTP-72-based car-following test simulation is conducted to verify our scheme. Several conclusions can be obtained from this study:

(1) The novel CFDM in this study is capable of retaining and reproducing naturalistic driving styles. This is quantitatively analyzed by A_{ESD} and further demonstrated based on the k-means cluster method. For

the city road, the A_{ESD} of mild, moderate, and aggressive drivers generally falls within the range of [220, 270], [280, 320], and [330, 400], respectively. And for the highway, these are [750, 870], [900, 990], and [1000, 1200], respectively.

(2) The CFDM can track the leading vehicle's speed quit well, and the error of relative distance is mostly less than 5 meters for every driving styles.

(3) The car-following accuracy is sensitive to B-spline function, and the driving style is not at all. The best performance is obtained when the order of B-spline function is 3 both for the city road and highway.

(4) The CFDM performance is consistent with the original driving data, where all of the $\sigma_{err(VS)}$ and $\sigma_{err(DR)}$ are small.

(5) Similar driving features are demonstrated by the same style of CFDMs; however, minor diversities exist even though of the same driving style.

The proposed scheme is a realistic approach based on the state of the art in car-following driving modeling. And it is suitable for the situation where human drivers are replaced by robot drivers and driving style is an important issue. In our future work, efforts will be devoted to driverless driving and the driving assistance system for safer driving when autonomous vehicles and human-operated vehicles coexist.

Notations

CFM: Car-following model
CFDM: Car-following driver model
CFD: Car-following data
STDM: Speed-tracking driver model
ESD: Energy spectrum density
DBD: Driving behavior data
VS: Vehicle speed
TP: Throttle position
BP: Brake pressure
SCD: Simulated car-following data
RCD: Real-world car-following data
*Vir*Driver: Virtual driver
DSC: Distance-to-speed conversion
THW: Time-headway.

Data Availability

The data used to support the findings of this study are available from the corresponding author upon request.

Conflicts of Interest

The authors declare that there are no conflicts of interest regarding the publication of this paper.

Acknowledgments

This research was supported in part by the National Key Research and Development Program of China under Grant 2018YFB1004900, in part by the Zhejiang Provincial Natural Science Foundation under Grant LQ18F030010 and Grant 2016C31117, and in part by the Project of Science and Technology Plans of Wenzhou under Grant G20170010 and Grant 2018ZG021.

References

[1] D. C. Gazis, R. Herman, and R. B. Potts, "Car-following theory of steady-state traffic flow," *Operations Research*, vol. 7, no. 4, pp. 499–505, 1959.

[2] P. G. Gipps, "A behavioural car-following model for computer simulation," *Transportation Research Part B: Methodological*, vol. 15, no. 2, pp. 105–111, 1981.

[3] E. Kometani and T. Sasaki, "Dynamic behavior of traffic with a nonlinear spacing-speed relationship," in *Theory Traffic Flow*, pp. 105–119, Elsevier Publishing Co., Amsterdam, Netherlands, 1961.

[4] S. Kikuchi and P. Chakroborty, "Car-following model based on fuzzy inference system," *Transportation Research Record*, vol. 1365, pp. 82–91, 1992.

[5] H. Jia, Z. Juan, and A. Ni, "Develop a car-following model using data collected by 'five-wheel system," in *Proceedings of the 2003 IEEE International Conference on Intelligent Transportation Systems*, vol. 1, pp. 346–351, Shanghai, China, October 2003.

[6] M. Brackstone and M. McDonald, "Car-following: a historical review," *Transportation Research Part F: Traffic Psychology and Behaviour*, vol. 2, no. 4, pp. 181–196, 1999.

[7] H.-H. Chiang, S.-J. Wu, J.-W. Perng, B.-F. Wu, and T.-T. Lee, "The human-in-the-loop design approach to the longitudinal automation system for an intelligent vehicle," *IEEE Transactions on Systems, Man, and Cybernetics—Part A: Systems and Humans*, vol. 40, no. 4, pp. 708–720, 2010.

[8] J. Wang, L. Zhang, D. Zhang, and K. Li, "An adaptive longitudinal driving assistance system based on driver characteristics," *IEEE Transactions on Intelligent Transportation Systems*, vol. 14, no. 1, pp. 1–12, 2013.

[9] S. Tak, S. Kim, D. Lee, and H. Yeo, "A comparison analysis of surrogate safety measures with car-following perspectives for advanced driver assistance system," *Journal of Advanced Transportation*, vol. 2018, Article ID 8040815, 14 pages, 2018.

[10] H. Zhao, R. He, and C. Ma, "An extended car-following model at signalised intersections," *Journal of Advanced Transportation*, vol. 2018, Article ID 5427507, 26 pages, 2018.

[11] M. Seraj, J. Li, and Z. Qiu, "Modeling microscopic car-following strategy of mixed traffic to identify optimal platoon configurations for multiobjective decision-making," *Journal of Advanced Transportation*, vol. 2018, Article ID 7835010, 15 pages, 2018.

[12] A. Loulizi, Y. Bichiou, and H. Rakha, "Steady-state car-following time gaps: an empirical study using naturalistic driving data," *Journal of Advanced Transportation*, vol. 2019, Article ID 7659496, 9 pages, 2019.

[13] E. R. Boer and M. Hoedemaeker, "Modeling driver behavior with different degrees of automation: a hierarchical décision framework of interacting mental models," in *Proceedings of the 17th European Annual Conference on Human Decision Making and Manual Control*, pp. 63–72, Valenciennes, France, December 1998.

[14] E. R. Boer, "Car following from the driver's perspective," *Transportation Research Part F: Traffic Psychology and Behaviour*, vol. 2, no. 4, pp. 201–206, 1999.

[15] R. X. Zhong, K. Y. Fu, A. Sumalee, D. Ngoduy, and W. H. K. Lam, "A cross-entropy method and probabilistic

sensitivity analysis framework for calibrating microscopic traffic models," *Transportation Research Part C: Emerging Technologies*, vol. 63, pp. 147–169, 2016.

[16] M. Zhu, X. Wang, and Y. Wang, "Human-like autonomous car-following model with deep reinforcement learning," *Transportation Research Part C: Emerging Technologies*, vol. 97, pp. 348–368, 2018.

[17] A. Khodayari, A. Ghaffari, R. Kazemi, and R. Braunstingl, "A modified car-following model based on a neural network model of the human driver effects," *IEEE Transactions on Systems, Man, and Cybernetics—Part A: Systems and Humans*, vol. 42, no. 6, pp. 1440–1449, 2012.

[18] Y. Qiu and R. Jia, "Adaptive hysteresis compensation of piezoelectric actuator using direct inverse modelling approach," *Micro & Nano Letters*, vol. 13, no. 2, pp. 180–183, 2018.

[19] L. Xu, J. Hu, H. Jiang, and W. Meng, "Establishing style-oriented driver models by imitating human driving behaviors," *IEEE Transactions on Intelligent Transportation Systems*, vol. 16, no. 5, pp. 2522–2530, 2015.

[20] B. Shi, L. Xu, J. Hu et al., "Evaluating Driving Styles by normalizing driving behavior based on personalized driver modeling," *IEEE Transactions on Systems, Man, and Cybernetics: Systems*, vol. 45, no. 12, pp. 1502–1508, 2015.

[21] P. Stoica, R. L. Moses, and P. Hall, "Introduction to spectral analysis," *Technometrics*, vol. 47, no. 1, pp. 104-105, 2005.

[22] D. Shinar and E. Schechtman, "Headway feedback improves intervehicular distance: a field study," *Human Factors: The Journal of the Human Factors and Ergonomics Society*, vol. 44, no. 3, pp. 474–481, 2002.

[23] W. V. Winsum and A. Heino, "Choice of time-headway in car-following and the role of time-to-collision information in braking," *Ergonomics*, vol. 39, no. 4, pp. 579–592, 1996.

[24] M. Saffarian, J. C. F. De Winter, and R. Happee, "Enhancing driver car-following performance with a distance and acceleration display," *IEEE Transactions on Human-Machine Systems*, vol. 43, no. 1, pp. 8–16, 2013.

[25] C.-F. Hsu and Y.-C. Chen, "Microcontroller-based B-spline neural position control for voice coil motors," *IEEE Transactions on Industrial Electronics*, vol. 62, no. 9, pp. 5644–5654, 2015.

[26] S. Chen, X. Hong, J. Gao, and C. J. Harris, "Complex-valued B-spline neural networks for modeling and inverting hammerstein systems," *IEEE Transactions on Neural Networks and Learning Systems*, vol. 25, no. 9, pp. 1673–1685, 2014.

[27] L. Pariota, F. Galante, and G. N. Bifulco, "The impact of the leading vehicle type on car-following behaviours," in *Proceedings of the 2015 International Conference on Models and Technologies for Intelligent Transportation Systems (MT-ITS)*, pp. 30–37, Budapest, Hungary, June 2015.

[28] Q. Ji, Z. Zhu, and P. Lan, "Real-time nonintrusive monitoring and prediction of driver fatigue," *IEEE Transactions on Vehicular Technology*, vol. 53, no. 4, pp. 1052–1068, 2004.